Heliyon 10 (2024) e39527

Contents lists available at ScienceDirect

Heliyon

journal homepage: www.cell.com/heliyon

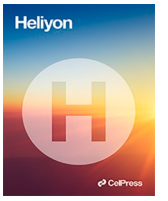

Research article

A digital twin approach for stroke risk assessment in Atrial Fibrillation Patients

Matteo Falanga [a,*], Camilla Cortesi [a], Antonio Chiaravalloti [b], Alessandro Dal Monte [b], Corrado Tomasi [b], Cristiana Corsi [a]

[a] DEI, University of Bologna, Campus of Cesena, Bologna, Italy
[b] Santa Maria delle Croci Hospital, AUSL della Romagna, Ravenna, Italy

ARTICLE INFO

Keywords:
Atrial fibrillation
Left atrium
Computational fluid dynamics
Thromboembolic risk

ABSTRACT

Atrial fibrillation (AF) is associated with a fivefold increased risk of cerebrovascular events, contributing to 15–18 % of all strokes. Stroke prevention in clinical practice is typically guided by the CHA_2DS_2-VASc score, which depends on general clinical risk factors but falls short in predicting risk at an individual patient level. In this study, we introduce a digital twin model of the left atrium (LA) combined with computational fluid dynamics (CFD) simulations to enhance personalized stroke risk assessment. Simulations were performed on patient-specific dynamic LA models in sinus rhythm (SR) across three patient groups: 10 controls (CTRL), 10 with paroxysmal AF (PAR-AF), and 10 with persistent AF (PER-AF). Blood flow velocity and areas susceptible to thrombogenesis, based on several factors including endothelial damage, were identified in the left atrial appendage (LAA). In general, control subjects exhibited higher average blood velocity in both the LAA and its ostium (0.11 ± 0.03 m/s and 0.28 ± 0.05 m/s, respectively) compared to those with AF. In the AF groups, the velocities were lower (LAA: PAR-AF 0.05 ± 0.02 m/s, PER-AF 0.04 ± 0.02 m/s; LAA ostium: PAR-AF 0.14 ± 0.03 m/s, PER-AF 0.11 ± 0.04 m/s). CFD analysis revealed that endothelial cell activation potential (ECAP) was significantly higher in AF patients (PAR-AF: 3.96 ± 3.28 Pa^{-1}, PER-AF: 4.77 ± 2.08 Pa^{-1}) compared to controls (0.93 ± 0.63 Pa^{-1}). These findings suggest that AF patients experience slower and more oscillatory blood flow in the LAA, increasing their risk of thrombosis. Additionally, blood tends to stagnate within the LAA, further raising the likelihood of clot formation. This proposed method could be used to enhance stroke risk stratification in AF patients by incorporating an index that integrates blood velocity-derived parameters.

1. Introduction

Atrial fibrillation (AF) is the most common form of arrhythmia globally, and its prevalence is expected to rise significantly in the near future due to population aging and improved survival rates in heart disease patients, which prolongs exposure to cardiovascular risk factors [1]. AF is associated with a well-established fivefold increase in the risk of cardioembolic events, but the underlying mechanisms of thrombogenesis in AF are complex and not fully understood. Virchow's triad remains the fundamental

* Corresponding author. Department of Electrical, Electronic and Information Engineering "Guglielmo Marconi" Via dell'Università 50, 47522, Cesena, FC, Italy.
E-mail address: matteo.falanga2@unibo.it (M. Falanga).

https://doi.org/10.1016/j.heliyon.2024.e39527
Received 7 May 2024; Received in revised form 14 October 2024; Accepted 16 October 2024
Available online 18 October 2024

pathophysiological framework: thrombus formation arises from coagulation abnormalities, tissue (atrial myocardium and endocardium) dysfunction, and altered blood flow dynamics within the atria. AF can affect all three components of Virchow's triad and consistently leads to damage in atrial cells and structures, including the LAA. This process, known as atrial remodeling, is characterized by progressive enlargement of the left atrium and LAA, increased tissue fibrosis, and reduced contractile strength of the atrial walls [2,3]. Because many episodes of AF are asymptomatic, it is challenging to accurately assess its overall contribution to both atrial cardiomyopathy and thrombogenesis. It is now hypothesized that in some cases, AF may merely serve as a marker of an underlying atrial cardiomyopathy, which itself can promote local thrombogenesis through alternative biological pathways, independently triggering Virchow's process.

Atrial remodeling is linked to an elevated risk of cardioembolic events and heart failure, though its progression can vary significantly due to several still partially understood factors. However, appropriate treatments can slow down or even reverse the remodeling process [4].

Clinical risk is typically assessed using widely adopted scoring systems, with the CHA_2DS_2-VASc score being the most common. This score is based on a limited set of general clinical descriptors, such as age, sex, hypertension, diabetes, congestive heart failure, and prior stroke, which were identified in large epidemiological studies. However, without a precise metric to evaluate the balance of Virchow's triad factors at the individual level, the CHA_2DS_2-VASc score is an imperfect predictor of stroke, offering only modest predictive accuracy and performing particularly poorly in distinguishing risk among low-risk patients. Other scoring systems have been proposed to enhance the classification of AF patients, such as the ATRIA (Anticoagulation and Risk Factors in Atrial Fibrillation) score [5], which has been shown to be more accurate than the CHA_2DS_2-VASc score in identifying low-risk patients. However, the calculation of the ATRIA score is also based on factors like age, history of stroke or transient ischemic attack, diabetes, hypertension, heart failure, proteinuria, and renal disease. These factors are assigned to specific point values that contribute to the final score [6]. Despite its improved performance, the ATRIA score still exhibits similar limitations in predictive accuracy when applied to individual patients [7].

The relationship between AF patterns and stroke risk, independent of $CHADS_2$ and CHA_2DS_2-VASc scores, is currently a topic of much debate. Understanding this link is complicated by evidence that patients with paroxysmal AF tend to have a different clinical profile compared to those with other forms of AF. Paroxysmal AF patients are typically younger, with a lower prevalence of structural heart disease and comorbidities such as chronic kidney disease, chronic obstructive pulmonary disease, and peripheral vascular disease. They also tend to have a lower estimated risk of thromboembolic events and bleeding [8,9]. In a meta-analysis by Zhang et al., examining chronic anticoagulation in patients at moderate-to-high stroke risk, it was found that paroxysmal AF patients who received treatment had significantly lower rates of stroke and all-cause mortality compared to those with non-paroxysmal AF. Importantly, the reduction in stroke risk among patients with paroxysmal AF was not linked to a decreased risk of hemorrhage, as the safety profile of anticoagulation therapy remained consistent across different types of AF [10]. This evidence highlights the necessity of conducting stroke risk assessments tailored to the individual patient's profile to enhance clinical outcomes and optimize resource allocation for AF management.

To develop a comprehensive patient-specific profile, computational fluid dynamics (CFD) simulations play a crucial role, in addition to the information typically available in clinical settings. These simulations enable detailed analysis of blood flow patterns within the heart, especially in the left atrial appendage (LAA), and provide valuable insights into regions prone to blood stasis, which increases the risk of clot formation.

Analyzing blood flow patterns within the LA and LAA using CFD simulations has been suggested as a novel method for identifying the mechanistic factors that contribute to atrial thrombogenesis at the individual level. The initial studies that utilized more generalized boundary conditions, like average flow rates, provided valuable insights into flow patterns; however, they did not possess the level of detail necessary for accurate individual risk stratification. More recent studies have shown that it is possible to simulate realistic three-dimensional blood flow patterns in LA by employing patient-specific dynamic anatomical models, incorporating LA displacement obtained from imaging data, and using boundary conditions derived from Doppler measurements at the pulmonary veins (PVs) and the mitral valve (MV) [11–13]. Sun et al. (2023) utilized advanced CFD models to improve thrombus risk predictions by analyzing factors such as Relative Residence Time (RRT) and Oscillatory Shear Index (OSI) [14]. A comparison of these findings reveals that the evolution of CFD simulations, from basic anatomical models and average flow rates to patient-specific dynamics and detailed boundary conditions, has significantly deepened our understanding of LA hemodynamics. This advancement carries practical implications for clinical practice, allowing for more precise identification of high-risk patients who could benefit from targeted anticoagulation therapy or interventional procedures to mitigate stroke risk [14,15].

Building on these advancements in CFD simulations for evaluating stroke risk in AF patients, we propose the creation of a digital twin (DT) of the LA and LAA. This digital twin would utilize patient-specific data to develop a dynamic, real-time model that accurately simulates blood flow patterns and predicts the risk of thrombus formation. By integrating anatomical data, flow conditions, and the mechanical properties of the atrial walls, the digital twin would serve as a comprehensive tool for personalized stroke risk assessment. This approach could enhance the accuracy of risk stratification and facilitate more tailored therapeutic interventions, ultimately leading to improved patient outcomes.

2. Methods

2.1. Study population

A total of one hundred patients were enrolled in the observational registry FATA ("Fluid-dynamics in the Left Atrium in Atrial

Fibrillation Patients and Controls for Thrombogenic Risk Analysis"), which was conducted by the Cardiology and Radiology Units at "S Maria delle Croci" Hospital in Ravenna, part of the Health Service of Romagna, Italy (approved by the Local Ethics Committee - C.E.R.O.M., approval no. 1276/2019 I.5/6, on February 13, 2019). The enrollment criteria included no history of prior arterial embolic events or strokes, no congenital heart disease, and no previous heart surgeries or percutaneous interventions, including any ablations for tachyarrhythmias. Among the enrolled patients, thirty non-consecutive individuals were selected and further categorized into three groups based on their clinical presentation of AF (Table 1).

2.2. Patients data acquisition

Contrast-Enhanced Computed Tomography (CECT) data were acquired using a Philips Brilliance 64 CT scanner while the patients were in sinus rhythm (SR). Ten volumes (comprising 170 axial slices with a pixel size of 0.4 mm and a slice thickness of 1 mm) were reconstructed to cover a full cardiac cycle, starting from the end of ventricular diastole, using retrospective ECG gating. The CECT files were saved in DICOM format, and Doppler measurements were also collected at the MV and PVs.

2.3. Data analysis

The data processing workflow utilized for the analysis is illustrated in Fig. 1. Details regarding the creation of the dynamic model and the execution of the CFD simulations can be found in the supplementary material [16–18].

The blood velocity fields at both the ostium and within the LAA were analyzed for each model. Furthermore, metrics such as time-average wall shear stress (TAWSS), oscillatory shear index (OSI), relative residence time (RRT), and endothelial cell activation potential (ECAP) were assessed in the LAA. These variables can also be used to evaluate how blood rheological methodologies influence the optimization of patient-specific left atrial appendage occlusion strategies for thrombosis assessment [19,20].

First, the viscous stress vector $\vec{\tau}$ exerted by the wall on the fluid is defined as follows:

$$\vec{\tau} = \mu \left[\nabla \vec{u} + (\nabla \vec{u})^T \right] \bullet \vec{n}$$

where μ represents the viscosity of blood, $\nabla \vec{u}$ denotes the velocity gradient, and $\vec{n}$ is the unit normal vector extending from the fluid to the wall.

In general, the normal component of the viscous stress vector can be subtracted from the total viscous stress vector to obtain the wall shear stress ($\overrightarrow{WSS}$) vector, including direction:

$$\overrightarrow{WSS} = \vec{\tau} - (\vec{\tau} \bullet \vec{n})\ \vec{n}$$

Wall shear stress quantifies the retarding force (per unit area) exerted by the left atrial endocardial wall on the layers of blood flowing adjacent to it. This stress reflects the shear traction generated by the blood flow acting on the endothelial cell surface. The wall's force on the fluid per unit area is represented by the WSS in a direction parallel to the local tangent plane. Due to the periodic nature of the heartbeat, it is possible to calculate an average metric known as TAWSS, which is defined as follows:

$$TAWSS = \frac{1}{T} \int_0^T \left\| \overrightarrow{WSS} \right\|_2 dt$$

where T represents the total duration of the simulated cardiac cycles, and $\| \bullet \|_2$ denotes the Euclidean norm of a vector. Consequently, TAWSS can offer insights into areas that promote thrombus deposition and growth.

Because WSS is calculated based on the magnitude of the shear force, it does not account for the oscillatory nature of the flow. Therefore, the OSI is introduced as follows:

$$OSI = \frac{1}{2} \left(1 - \frac{\left\| \int_0^T \overrightarrow{WSS}\, dt \right\|_2}{\int_0^T \left\| \overrightarrow{WSS} \right\|_2 dt} \right)$$

Table 1
Main characteristics of the patients in the three groups (CTRL: control, PAR-AF: paroxysmal AF, PER-AF: persistent AF). BSA: Body Surface Area; LV EF: Left Volume Ejection Fraction; LA: left Atrium; Mitral Valve Regurgitation: 0: no regurgitation, 1: minimal, 2: mild, 3: moderate, 4: severe; ^p < 0.05 CTRL vs PAR-AF and PER-AF.

	CTRL	PAR-AF	PER-AF
Gender (M/F)	7M/3F	8M/2F	8M/2F
Age (years)	58 ± 12	60 ± 8	67 ± 9
BSA (m^2)	1.9 ± 0.2	2.0 ± 0.1	2.0 ± 0.2
LV EF (%)	58.5 ± 3.2	57.0 ± 10.8	57.5 ± 3.4
Normalized LA volume (ml/m^2)	45.3 ± 10.0^	60.6 ± 11.0	79.6 ± 16.1
Mitral Valve Regurgitation (0 ÷ 4)	0.1 ± 0.3^	1.1 ± 1.0	1.4 ± 1.0

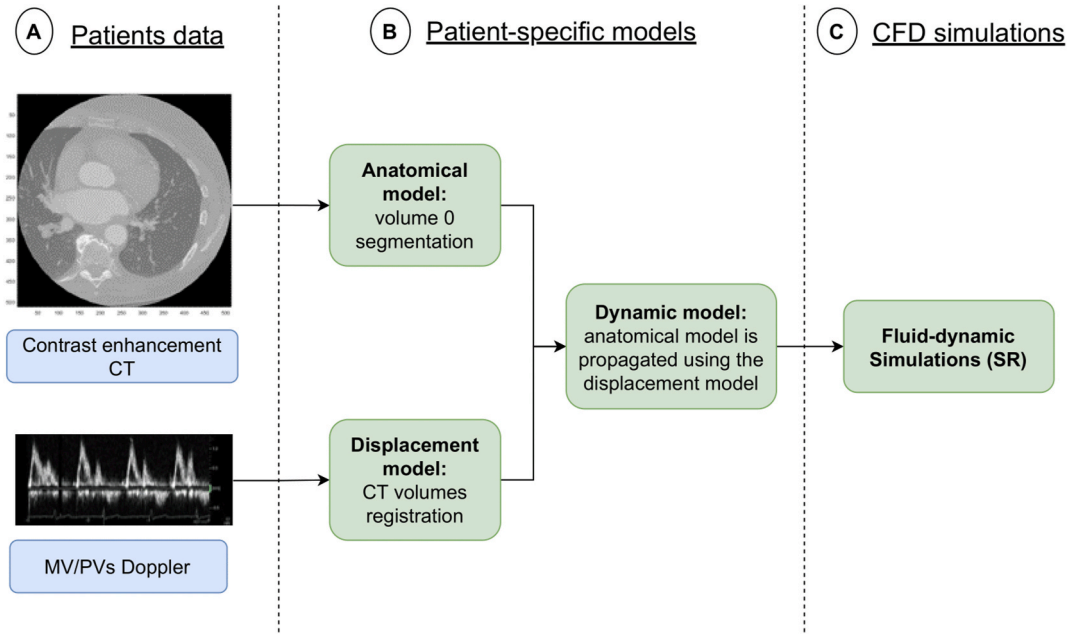

Fig. 1. Graphical description of the workflow designed for the analysis: patient-specific contrast enhanced CT (CECT) data are segmented and registered to derive the LA anatomical model and the 3D displacement fields allowing to derive the LA dynamic model representing the computational domain for the CFD simulation in sinus rhythm (SR) using mitral valve/pulmonary veins (MV/PVs) Doppler as boundary conditions.

OSI characterizes the deviation of the WSS vector from its average direction; a higher OSI value indicates greater oscillation in the flow. This dimensionless metric ranges from [0, 0.5] and is elevated in areas where the WSS fluctuates significantly throughout the cardiac cycle. The directional changes in flow primarily contribute to the higher OSI values.

RRT represents the duration that blood spends close to the left atrial wall. It describes the accumulation of inflammatory cells, which can lead to degradation of the LA wall, potentially resulting in enlargement and particle deposition. RRT is defined as follows:

$$RRT = \frac{1}{(1 - 2OSI)^{*}TAWSS}$$

This indicator identifies regions of the wall where shear stress is low and the flow is oscillatory. The duration of blood residence near the wall increases in this hemodynamic environment. Such conditions may facilitate particle deposition and trigger an inflammatory response in the endothelial cells.

To identify areas of the wall that experience both high OSI and low TAWSS, Di Achille et al. [21] proposed a new index that uses the ratio of these two indices to assess the degree of 'thrombogenic susceptibility' of the wall. This metric is known as ECAP:

$$ECAP = \frac{OSI}{TAWSS}$$

Higher values of the ECAP index are associated with conditions of elevated OSI and reduced TAWSS, indicating increased endothelial susceptibility. This measure is commonly used in studies assessing thrombogenic risk within the LAA [22,23].

Additionally, to assess blood stasis, the residence time T_r is defined as the duration that blood particles remain within the LA chamber. This quantity is expressed by the following equation:

$$\frac{\partial T_r}{\partial t} + \vec{v}^{*}\nabla T_r = 1$$

Rather than solving the equation directly, the 3D flow velocity field generated from the simulation was utilized to track the Lagrangian flow tracers, allowing for the estimation of the time elapsed along their paths. Subsequently, the spatio-temporal evolution of blood residence time within the LAA was assessed. It is noted that, despite potential numerical errors, this method yields results that are essentially equivalent to solving the equation directly [24].

2.4. Statistical analysis

The parameters outlined earlier were calculated for all participants enrolled in the study, and comparisons between the groups were made. To evaluate the normal distribution of each parameter, a one-sample Kolmogorov-Smirnov test was first conducted among the three groups. As all parameters demonstrated a normal distribution, the data are presented as mean ± standard deviation. A one-

way ANOVA was then performed to determine any statistical differences among the groups. Statistical significance was established with a p-value of less than 0.05.

3. Results

In all study subjects, data processing and simulations were successful, allowing for comprehensive analysis.

3.1. Blood velocity

The results revealed significant differences in average velocity values among the different groups within the LA. Specifically, control subjects exhibited substantially higher average velocities compared to those with AF. The recorded average velocities were 0.5 $\pm$ 0.12 m/s for control subjects, 0.2 $\pm$ 0.05 m/s for PAR-AF subjects, and 0.07 $\pm$ 0.01 m/s for PER-AF subjects. These differences underscore the variations in flow dynamics between the groups, with control subjects demonstrating markedly higher blood flow speeds.

When examining blood velocity within the LAA, the data exhibited considerable variability. The lowest mean velocity was recorded in a PER-AF subject at 0.02 m/s, indicating very slow blood flow. In contrast, the highest mean velocity was observed in a control subject, at 0.18 m/s. On average, the control group showed a higher mean velocity (0.12 $\pm$ 0.03 m/s) compared to the PAR-AF group (0.05 $\pm$ 0.02 m/s) and the PER-AF group (0.04 $\pm$ 0.02 m/s), with statistical significance ($p < 0.05$) (Table 2). This suggests that control subjects experienced more robust blood flow within the LAA, which may be linked to more efficient cardiac function.

Further analysis focused on the mean velocity at the LAA ostium. The results indicated that the control group had a significantly higher average velocity (0.28 $\pm$ 0.05 m/s) compared to both the PAR-AF group (0.14 $\pm$ 0.03 m/s) and the PER-AF group (0.11 $\pm$ 0.04 m/s), with statistical significance ($p < 0.05$) (Table 3). This higher velocity at the LAA ostium in control subjects suggests more effective blood flow and potentially improved washout during the cardiac cycle. The enhanced washout observed in control subjects could indicate better overall atrial function and a reduced risk of thrombus formation.

For a detailed overview of patient-specific velocity values and statistical analyses, refer to Tables 2 and 3.

3.2. TAWSS, OSI, RRT and ECAP

In Fig. 2, TAWSS, OSI, RRT and ECAP maps in the LAA in a representative subject for each group are shown.

As reported in Table 4, our analysis revealed that control subjects exhibited higher TAWSS values at the LAA ostium compared to subjects with AF. Specifically, the average TAWSS across the entire LAA was 0.78 $\pm$ 0.35 Pa for control subjects. In contrast, PAR-AF and PER-AF subjects had lower average TAWSS values of 0.28 $\pm$ 0.16 Pa and 0.18 $\pm$ 0.07 Pa, respectively ($p < 0.05$). This suggests that the velocity gradient and associated wall shear stress were generally higher in control subjects, which could indicate more effective blood flow dynamics in the absence of AF.

OSI values, which reflect the variability in blood flow direction, were notably higher in AF subjects compared to controls. Specifically, PAR-AF and PER-AF subjects had OSI values of 0.25 $\pm$ 0.06 and 0.22 $\pm$ 0.06, respectively, while control subjects had an OSI value of 0.20 $\pm$ 0.07. These elevated OSI values in AF patients are likely due to the altered blood flow patterns in the LAA, where the flow direction reverses significantly during a heartbeat. This phenomenon results in greater fluctuations in flow direction, particularly at the tip of the appendage. However, the differences in OSI between groups were not statistically significant ($p = 0.2$), indicating that while observable trends exist, they may not be substantial enough to draw definitive conclusions.

RRT, which measures the duration that blood particles spend near the wall, was significantly higher in the PAR-AF and PER-AF groups (123.83 $\pm$ 143.68 Pa^{-1} and 112.79 $\pm$ 97.25 Pa^{-1}, respectively) compared to the control group (9.09 $\pm$ 7.66 Pa^{-1}) ($p < 0.05$). This suggests that subjects with AF experience higher oscillatory flow, which is associated with prolonged wall contact. Such extended contact may increase the risk of particle deposition and potential inflammatory responses in the endothelial cells lining the

Table 2
Mean velocity values in the LAA for each patient in each group and average value for the entire group (last row). ^$p < 0.05$ CTRL vs PAR-AF and PER-AF.

Mean LAA velocity (m/s)		
CTRL	PAR-AF	PER-AF
0.09	0.05	0.03
0.09	0.03	0.03
0.13	0.06	0.02
0.13	0.05	0.05
0.08	0.02	0.06
0.11	0.06	0.02
0.12	0.06	0.04
0.18	0.07	0.06
0.08	0.04	0.07
0.14	0.07	0.03
0.12 $\pm$ 0.03^	**0.05 $\pm$ 0.02**	**0.04 $\pm$ 0.02**

Table 3
Mean velocity values of the LAA ostium for each patient in each group and average value for the entire group (last row). ˆp < 0.05 CTRL vs PAR-AF and PER-AF.

Mean LAA ostium velocity (m/s)		
CTRL	PAR-AF	PER-AF
0.25	0.12	0.1
0.21	0.09	0.1
0.29	0.16	0.08
0.32	0.17	0.13
0.24	0.1	0.15
0.25	0.13	0.01
0.29	0.14	0.12
0.35	0.18	0.13
0.21	0.09	0.15
0.35	0.18	0.1
0.28 ± 0.05ˆ	**0.14 ± 0.03**	**0.11 ± 0.04**

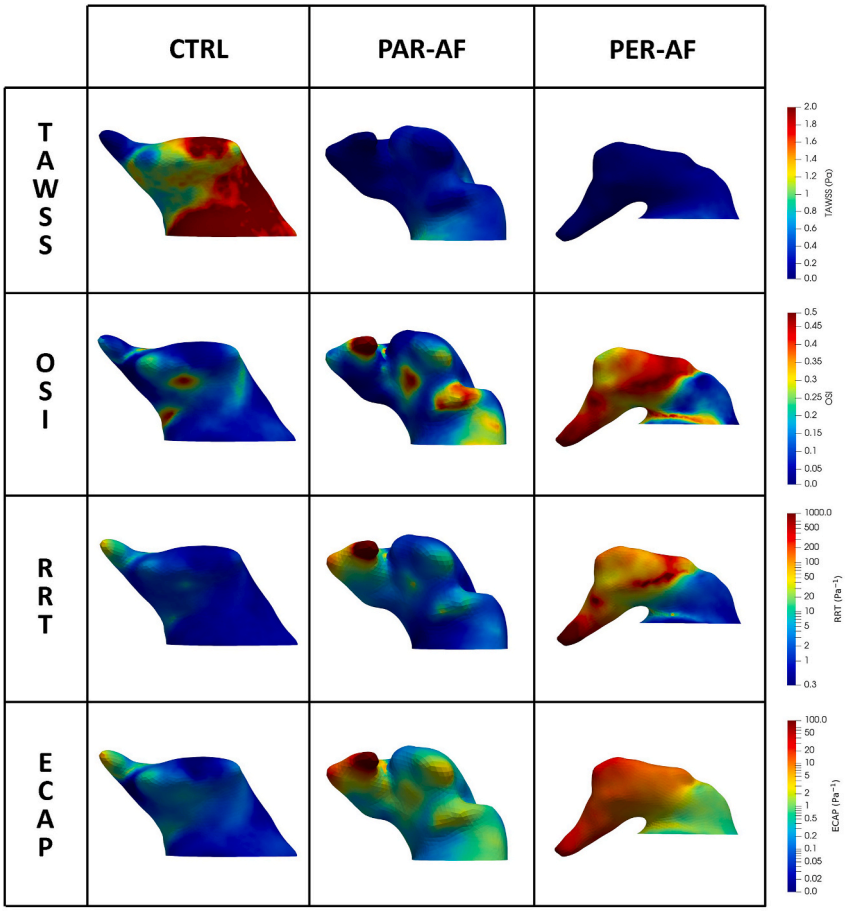

Fig. 2. CFD-derived parameters (Time-Averaged Wall Shear Stress throughout the cardiac cycle in the 1st row; Oscillatory Shear Index in the 2nd row; Relative Residence Time in the 3rd row; Endothelial Cell Activation Potential in the 4th row) in one representative subject for each group (CTRL subject in the 1st column; a PAR-AF patient in the 2nd column; a PER-AF subject in the 3rd column).

blood vessels.

ECAP values, which indicate areas with a potential for thrombus formation, were significantly higher in the PAR-AF and PER-AF groups (3.96 ± 3.28 Pa^{-1} and 4.77 ± 2.08 Pa^{-1}, respectively) compared to the control group (0.93 ± 0.63 Pa^{-1}) ($p < 0.05$). These elevated ECAP values in subjects with AF suggest the presence of potentially thrombogenic areas, highlighting an increased risk of clot formation in the LAA of patients with AF.

The box plots of the CFD parameters, shown in Fig. 3, visually represent the data distribution across the different groups. These

Table 4
Mean values of the CFD-derived parameters in the LAA for each group (*CTRL vs PAR-AF and PER-AF).TAWSS: time-averaged wall shear stress; OSI: oscillatory stress index; RRT: Relative residence time; ECAP: endothelial cell activation potential.

Parameters	CTRL	PAR-AF	PER-AF	p-value*
TAWSS (Pa)	0.78 ± 0.35	0.28 ± 0.16	0.18 ± 0.07	<0.05
OSI	0.20 ± 0.07	0.22 ± 0.06	0.25 ± 0.06	0.2
RRT (Pa^{-1})	9.09 ± 7.66	123.83 ± 143.68	112.79 ± 97.25	<0.05
ECAP (Pa^{-1})	0.93 ± 0.63	3.96 ± 3.28	4.77 ± 2.08	<0.05

plots provide a clear and intuitive way to interpret the variability and trends in the previously discussed results. By illustrating the range, median, and any potential outliers within each group, the box plots facilitate accessible comparisons of the CFD parameters, making it easier to identify patterns and differences among the groups.

Fig. 4 illustrates the residence time T_r by showcasing a representative subject from each group. Overall, the lowest Tr values were recorded near the pulmonary veins inlets, where blood enters the left atrium, and velocities reach moderate levels of approximately 70–80 cm/s. This finding aligns with previous research by Durán et al. [22], which suggests that secondary flow patterns, running parallel to the mitral valve ostium, are less constrained by overall mass conservation within the chamber compared to primary flow patterns, which are perpendicular to the mitral valve ostium. Consequently, secondary flow patterns can vary significantly based on anatomical characteristics, boundary conditions, and other influencing factors. Importantly, changes in secondary flow patterns near the left atrial appendage ostium can substantially impact the flow within the appendage, thereby affecting the residence time in that region. In contrast, the washout process within the left atrial body is primarily governed by the main flow patterns.

When examining residence time within the left atrial body, there were no significant differences among the groups, with T_r values consistently around 1 s, corresponding to one cardiac cycle. Despite the impaired atrial activity in subjects with atrial fibrillation, T_r within the left atrial body rarely exceeded 2 cycles. Previous studies [13,23] have demonstrated that residence time is generally much longer within the left atrial appendage compared to the left atrial body. Additionally, while T_r in the left atrial body remained relatively uniform, the left atrial appendage exhibited considerable variation between normal and atrial fibrillation subjects. In normal subjects, T_r remained close to 1 cycle within the LAA, whereas in paroxysmal atrial fibrillation, T_r extended to 5 cycles at the tip of the appendage, and it was even longer in persistent atrial fibrillation. Notably, there was significant heterogeneity in T_r distribution within the proximal regions of the left atrial appendage, particularly among subjects with atrial fibrillation. This pattern was consistent across all subjects in each group.

To further investigate these dynamics, a linear regression model was applied to compare both TAWSS and ECAP with residence time within the LAA, as shown in Fig. 5. The results suggest an inverse relationship between T_r and TAWSS: as TAWSS increases, T_r

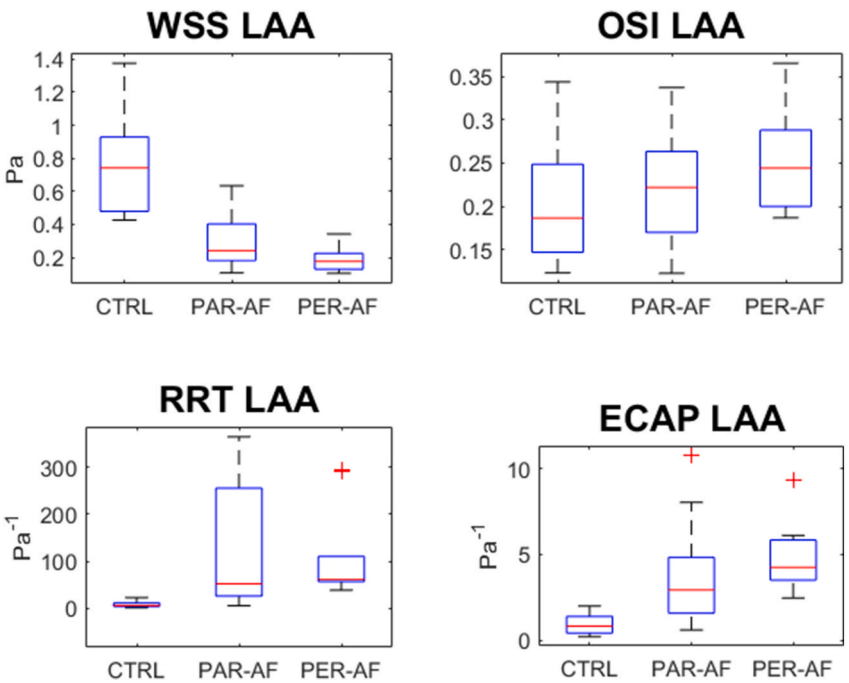

Fig. 3. Box plots of the computed CFD-derived parameters in the LAA in the three groups (CTRL, PAR-AF and PER-AF). Top left panel: Wall Shear Stress; Top right panel: Oscillatory Shear Index; Bottom left panel: Relative Residence Time; Bottom right panel: Endothelial Cell Activation Potential).

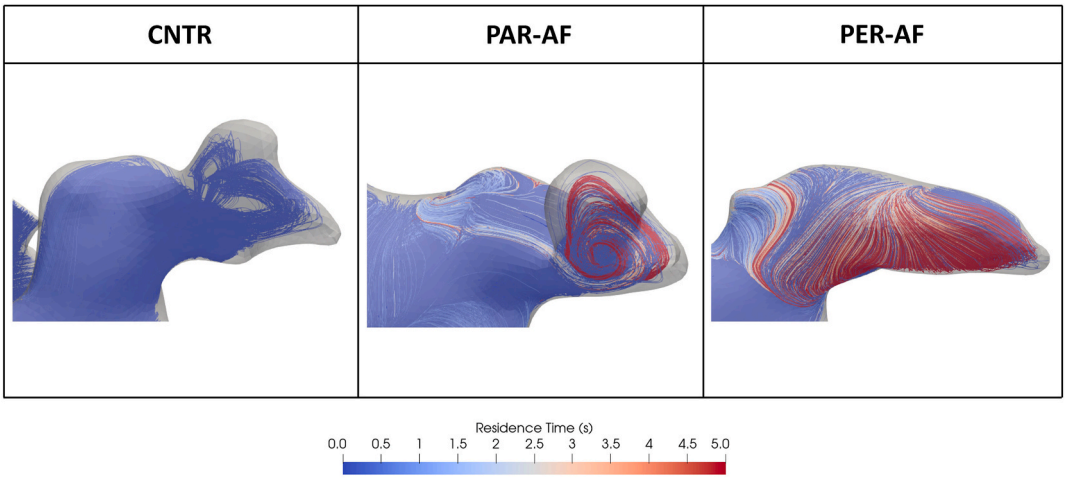

Fig. 4. Residence time representation in one representative subject for each group.

tends to decrease, displaying a consistent trend across all groups. This can be attributed to the fact that TAWSS is directly related to blood velocity; higher velocities contribute to more effective washout, thereby reducing T_r in those regions. Conversely, a positive correlation between T_r and ECAP was observed. As ECAP increases, T_r also increases, indicating that areas with higher potential for thrombogenesis are associated with longer residence times. This relationship underscores the heightened sensitivity of the hemodynamic environment in the LAA, particularly in subjects with atrial fibrillation, where the LAA is more reactive to changes compared to normal subjects. This increased sensitivity in patients with atrial fibrillation highlights the importance of closely monitoring these regions for potential thrombus formation.

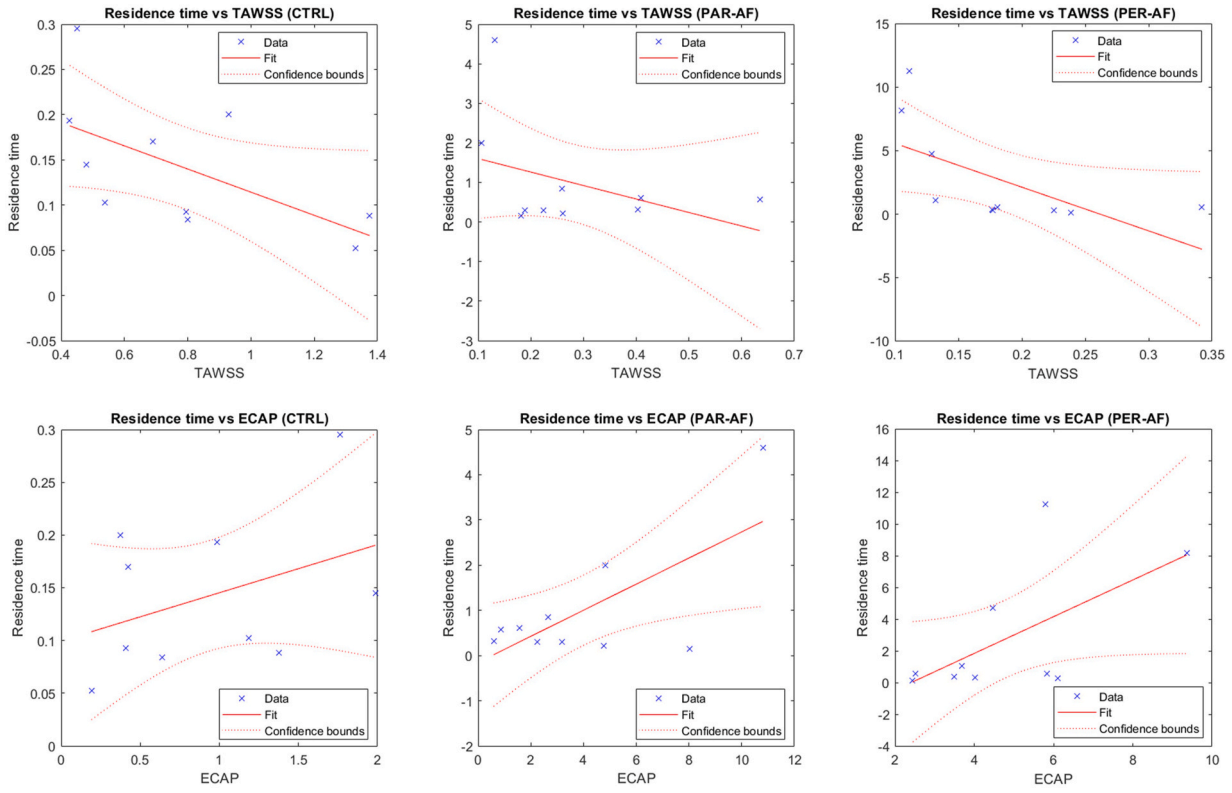

Fig. 5. Linear regression model between residence time T_r and TAWSS (top panels) and T_r and ECAP (bottom panels) in the three study groups (CTRL subjects – left panels, PAR-AF - mid panels, PER-AF - right panels PER).

4. Discussion

The proposed approach has demonstrated feasibility across all study subjects, offering a solid framework for the quantitative assessment of various hemodynamic parameters that can characterize stroke risk in patients with AF.

Computed hemodynamic parameters are widely utilized to examine how hemodynamics influence tissue mechanics in abdominal aortic diseases [25]. However, their application in patients with atrial fibrillation is limited to a few studies. Furthermore, directly comparing these values across different studies poses challenges due to several factors: (1) various studies employ different computational fluid dynamics models with distinct boundary conditions; (2) the calculation of these parameters is complex and necessitates a solid understanding of their physical significance; (3) not all computational fluid dynamics solvers automatically compute these parameters during hemodynamic simulations.

In J. Dueñas-Pamplona et al. study [23], a set of hemodynamic indices was evaluated within the LAA to compare flexible and rigid atrial models under fibrillation conditions. All parameters, with the exception of time-averaged wall shear stress, fell within the range observed in the control group.

In recent years, endothelial cell activation potential has been measured from blood velocity fields in studies [21,26,27]. Unfortunately, these investigations did not focus on developing a DT model for stroke risk assessment but rather examined the effects of specific heart rhythm issues or treatments. Thus, comparisons with our findings can only be qualitative. Nonetheless, the upward trend in ECAP values when comparing left atrial appendages in control subjects and those with atrial fibrillation is supported.

When comparing our results with those of Morales et al. [28] and Qureshi et al. [[27], we found similar ECAP values, even though these studies employed different computational fluid dynamics models and methodologies. In contrast, the ECAP values reported by Paliwal et al. [29] were significantly different.

Regarding residence time, although it was calculated by tracking Lagrangian flow tracers, similar values were reported by García-Villalba et al. [13] and Durán et al. [22]. The substantial difference in LAA velocity across groups is consistent with the higher T_r observed in our study among patients with AF. This finding may also explain the greater variability of T_r in this group's LAA in relation to ECAP.

The key finding of our study is that, on average, WSS was consistently lower, while OSI, ECAP, and RRT were consistently higher in the LAA of patients with AF compared to control subjects. Significant differences were observed for WSS, RRT and ECAP (Table 3). These results suggest that in patients with AF, the LAA is more susceptible to slower and more fluctuating blood flow than in controls.

In vitro studies have shown that exposure to such low and oscillating flow conditions can activate endothelial cells and promote a proinflammatory state [30]. Consequently, the combination of low WSS and high OSI may stimulate the endothelial cell layer of the LAA wall, attracting local platelets and leukocytes [31]. This process can activate the coagulation cascade near the endothelial cells through mechanisms similar to those seen in venous thrombus formation [32], ultimately leading to the development of a local clot. The clinical significance of these findings is that patients with AF are at a heightened risk for thromboembolic events, particularly strokes, due to the increased likelihood of clot formation within the LAA.

To implement this approach in clinical practice, patients would undergo imaging techniques such as contrast-enhanced computed tomography, magnetic resonance imaging, or real-time three-dimensional echocardiography to acquire detailed data of the LA and LAA. The imaging data would be processed using the developed two-dimensional segmentation technique to create an accurate anatomical model of the patient's left atrium and left atrial appendage. This step could be integrated into the standard radiology workflow, with specialized software managing the segmentation and model generation.

Using the anatomical model, CFD simulations would be conducted to calculate key hemodynamic parameters, including WSS, OSI, RRT and ECAP. These parameters would provide a quantitative assessment of the patient's stroke risk, particularly in relation to thrombus formation within the LAA. The results from the simulations would then be integrated into the patient's clinical profile alongside traditional stroke risk assessment tools, such as the CHA_2DS_2-VASc score.

This combined approach would enable clinicians to stratify patients based on their individual risk and tailor anticoagulation therapy accordingly. For instance, patients identified with particularly high-risk hemodynamic profiles might benefit from more aggressive anticoagulation strategies, closer monitoring, or even interventional procedures like left atrial appendage closure.

The integration of this advanced hemodynamic assessment into clinical practice marks a significant advancement in the personalization of stroke prevention strategies for patients with AF. Unlike traditional risk scores that provide general estimates based on population-level data, this approach facilitates precise evaluation of stroke risk on an individual basis. By incorporating patient-specific anatomical and hemodynamic data, clinicians can make more informed decisions regarding anticoagulation therapy, potentially reducing the risk of both stroke and bleeding complications.

To achieve this aim, we must address several challenges in both imaging and modeling. Cardiac imaging is a crucial method for assessing blood clot risk in patients with atrial fibrillation. However, transesophageal echocardiography (TEE), which is considered the gold standard for identifying thrombus in the left atrial appendage and demonstrates a sensitivity and specificity of 95 %–100 % clotting process at the vessel and coagulative status levels [33,34].

By incorporating additional metrics such as residence time in specific areas, vorticity, and kinetic energy [13,35], we can mitigate certain limitations. Some studies have proposed a blood hypercoagulability index using a simplified system of reaction-diffusion-convection equations to model thrombus growth dynamics. This approach focuses on key proteins in the blood clotting process, including thrombin, fibrinogen, and fibrin [26]. Our approach would significantly benefit from incorporating these additional indicators to enhance our understanding of how each factor influences stroke risk.

Utilizing a broader range of indices will enable us to explain the phenomenon of clot formation from multiple research perspectives, such as blood flow conditions, tissue injuries, and the creation and placement of particles. By weighing each factor appropriately, we

could develop a new clinical score to evaluate stroke risk on a patient-specific basis. However, it is important to recognize several limitations of this study. First, the relatively small sample size of 30 patients may restrict the generalizability of the findings. Larger size multicenter studies are necessary to validate these results across diverse populations and to confirm that the observed trends hold true across various patient demographics and clinical settings. Additionally, this study does not include long-term follow-up data, limiting our understanding of how these hemodynamic parameters may evolve over time and how they correlate with actual stroke outcomes in patients with atrial fibrillation. Longitudinal studies would be beneficial for assessing the predictive value of these parameters and for informing long-term management strategies for these patients.

Furthermore, the ability to quantitatively evaluate parameters such as residence time, vorticity, and kinetic energy in the LAA could facilitate the development of new clinical scores that are more sensitive and specific to the risk of thrombus formation in patients with AF. This advancement could enhance the identification of high-risk individuals who may benefit from preventive measures beyond standard anticoagulation, including catheter ablation or surgical interventions. Further research is required to validate these findings in larger, more diverse cohorts and to refine computational models for improved accuracy. Additionally, there is an opportunity to broaden the range of hemodynamic parameters considered in risk assessments. For instance, integrating metrics associated with blood hypercoagulability, such as those derived from reaction-diffusion-convection models of thrombus growth, could strengthen the predictive capabilities of these models. By gaining insights into the interplay between blood flow dynamics, tissue injuries, and coagulation processes, we can create a more comprehensive understanding of stroke risk in patients with AF.

To sum up, this approach has the potential to transform the management of patients with AF by offering a more comprehensive understanding of individual stroke risk and facilitating truly personalized medicine. By broadening the array of tools available to clinicians, we can advance towards the goal of preventing strokes more effectively and with greater precision, ultimately enhancing outcomes for patients with AF.

5. Conclusions

In conclusion, these preliminary findings indicate significant differences between patients diagnosed with AF and individuals without AF or relevant heart disease. The proposed method has the potential to develop a digital twin model for evaluating stroke risk in patients with AF. Ongoing tests on a larger sample population are being conducted in our lab, along with the assessment of various measurements through our computations. It is essential to pursue these steps to validate the initial findings and determine the risk level associated with each patient.

CRediT authorship contribution statement

Matteo Falanga: Writing – original draft, Visualization, Validation, Software, Methodology, Investigation, Formal analysis, Conceptualization. **Camilla Cortesi:** Visualization, Methodology, Formal analysis, Conceptualization. **Antonio Chiaravalloti:** Data curation. **Alessandro Dal Monte:** Data curation. **Corrado Tomasi:** Writing – review & editing, Investigation, Data curation, Conceptualization. **Cristiana Corsi:** Writing – review & editing, Visualization, Validation, Supervision, Resources, Project administration, Methodology, Funding acquisition, Formal analysis, Conceptualization.

Data availability statement

The data used in our study are not deposited in a publicly accessible repository, but they will be made available upon request.

Ethical approval statement

Data used in this study were acquired within the FATA project, approved by the Ethics IRST, IRCCS AVR Committee (CEIIAV n. 1456 prot.6076/2015 I.5/220). All subjects gave written informed consent in accordance with the Declaration of Helsinki.

Declaration of competing interest

The authors declare that they have no known competing financial interests or personal relationships that could have appeared to influence the work reported in this paper.

Acknowledgments

This work was supported by the Italian Ministry of University and Research (Italian National Project, PRIN2017 (‘Modeling the heart across the scales’).

The research leading to these results has received funding from the European Union - NextGenerationEU through the Italian Ministry of University and Research under PNRR - M4C2-I1.3 Project PE_00000019 "HEAL ITALIA" to DEI CUP J33C22002920006. The views and opinions expressed are those of the authors only and do not necessarily reflect those of the European Union or the European Commission. Neither the European Union nor the European Commission can be held responsible for them.”

Appendix A. Supplementary data

Supplementary data to this article can be found online at https://doi.org/10.1016/j.heliyon.2024.e39527.

References

[1] J. Kornej, C.S. Börschel, E.J. Benjamin, R.B. Schnabel, Epidemiology of atrial fibrillation in the 21st century: novel methods and new insights, Circ. Res. 127 (1) (2020) 4–20.

[2] D.K. Gupta, A.M. Shah, R.P. Giugliano, C.T. Ruff, E.M. Antman, L.T. Grip, et al., Left atrial structure and function in atrial fibrillation: engage af-timi 48, Eur. Heart J. 35 (22) (2014) 457–1465.

[3] L. Di Biase, P. Santangeli, M. Anselmino, P. Mohanty, I. Salvetti, S. Gili, et al., Does the left atrial appendage morphology correlate with the risk of stroke in patients with atrial fibrillation?: results from a multicenter study, J. Am. Coll. Cardiol. 60 (6) (2012) 531–538.

[4] S. Yaghi, C. Song, W.A. Gray, K.L. Furie, M.S. Elkind, H. Kamel, Left atrial appendage function and stroke risk, Stroke 46 (12) (2015) 3554–3559.

[5] D.E. Singer, Y. Chang, et al., A new risk scheme to predict ischemic stroke and other thromboembolism in atrial fibrillation: the ATRIA study stroke risk score, J. Am. Heart Assoc. 21 (2) (2013), 3.

[6] H.A. van den Ham, O.H. Klungel, D.E. Singer, H.G. Leufkens, T.P. van Staa, Comparative performance of ATRIA, CHADS2, and CHA2DS2-VASc risk scores predicting stroke in patients with atrial fibrillation: results from a national primary care database, J. Am. Coll. Cardiol. 27 (66) (2015) 1851–1859, 17.

[7] J.J.V. McMurray, Al. And the ESC committee for practice guidelines, "ESC guidelines for the diagnosis and treatment of acute and chronic heart failure 2012: the task force for the diagnosis and treatment of acute and chronic heart failure 2012 of the European society of Cardiology. Developed in collaboration with the heart failure association (HFA) of the ESC", Eur. Heart J. 33 (14) (2012) 1787–1847.

[8] G. Boriani, I. Laroche, I. Diemberger, et al., "'Real world' management and outcomes of patients with paroxysmal versus non-paroxysmal atrial fibrillation in europe: the EURObservational research programme–atrial fibrillation (EORP-AF) general pilot registry", Europace 18 (2016) 648–657.

[9] G.L. Botto, G. Tortora, M.C. Casale, F.L. Canevese, F.A.M. Brasca, Impact of the pattern of atrial fibrillation on stroke risk and mortality, Arrhythm Electrophysiol Rev 10 (2) (2021) 68–76.

[10] W. Zhang, Y. Xiong, L. Yu, et al., Meta-analysis of stroke and bleeding risk in patients with various atrial fibrillation patterns receiving oral anticoagulation, Am. J. Cardiol. 123 (2019) 922–928.

[11] A. Masci, M. Alessandrini, D. Forti, F. Menghini, L. Dedè, C. Tomasi, A. Quarteroni, C. Corsi, A proof of concept for computational fluid dynamic analysis of the left atrium in atrial fibrillation on a patient-specific basis, J. Biomech. Eng. 142 (1) (2020) 011002.

[12] J. Mill, V. Agudelo, C. Hion Li, J. Noailly, X. Freixa, O. Camara, D. Arzamendi, Patient-specific flow simulation analysis to predict device-related thrombosis in left atrial appendage occluders, REC Interv Cardiol 3 (4) (2021) 278–285.

[13] M. García-Villalba, L. Rossini, A. Gonzalo, D. Vigneault, P. Martinez-Legazpi, E. Durán, O. Flores, J. Bermejo, E. McVeigh, A.M. Kahn, J.C. Del Álamo, Demonstration of patient-specific simulations to assess left atrial appendage thrombogenesis risk, Front. Physiol. 12 (2021 Feb 26) 596596, https://doi.org/10.3389/fphys.2021.596596.

[14] J. Yang, Z. Bai, C. Song, H. Ding, M. Chen, J. Sun, X. Liu, Research on the internal flow field of left atrial appendage and stroke risk assessment with different blood models, Bioengineering 10 (2023) 944, https://doi.org/10.3390/bioengineering10080944.

[15] S. Valvez, M. Oliveira-Santos, A.P. Piedade, L. Gonçalves, A.M. Amaro, Computational flow dynamic analysis in left atrial appendage thrombus formation risk: a review, Appl. Sci. 13 (2023) 8201, https://doi.org/10.3390/app13148201.

[16] A. Masci, M. Alessandrini, D. Forti, F. Menghini, L. Dedé, C. Tomasi, A. Quarteroni, C. Corsi, A proof of concept for computational fluid dynamic analysis of the left atrium in atrial fibrillation on a patient-specific basis, J. Biomech. Eng. 1 (142) (2020) 011002, https://doi.org/10.1115/1.4044583. PMID: 31513697.

[17] S. Klein, M. Staring, K. Murphy, M.A. Viergever, J. P, W. Pluim, "Elastix: a toolbox for intensity-based medical image registration", IEEE Trans. Med. Imag. 29 (1) (2010) 196–205.

[18] P.C. Africa, Lifex: a flexible, high performance library for the numerical solution of complex finite element problems, SoftwareX 20 (2022) 101252.

[19] C. Albors, A. Olivares, X. Iriart, H. Cochet, J. Mill, O. Camara, Impact of blood rheological strategies on the optimization of patient-specific LAAO configurations for thrombus assessment, in: Functional Imaging and Modeling of the Heart, 2023, pp. 485–494.

[20] C. Albors, J. Mill, A. Olivares, X. Iriart, H. Cochet, O. Camara, Impact of Occluder Device Configurations in In-Silico Left Atrial Hemodynamics for the Analysis of Device-Related Thrombus, 2024.

[21] P. Di Achille, G. Tellides, C.A. Figueroa, J.D. Humphrey, A haemodynamic predictor of intraluminal thrombus formation in abdominal aortic aneurysms, Proceedings of the Royal Society A 470 (217) (2014).

[22] E. Durán, M. García-Villalba, P. Martínez-Legazpi, A. Gonzalo, E. McVeigh, A.M. Kahn, J. Bermejo, O. Flores, J.C. del Álamo, Pulmonary vein flow split effects in patient-specific simulations of left atrial flow, Comput. Biol. Med. 163 (2023).

[23] J. Dueñas-Pamplona, J.G. García, J. Sierra-Pallares, C. Ferrera, R. Agujetas, J.R. López-Mínguez, A comprehensive comparison of various patient-specific CFD models of the left atrium for atrial fibrillation patients, Comput. Biol. Med. 133 (2021).

[24] L. Rossini, P. Martinez-Legazpi, V. Vu, L. Fernandez-Friera, et al., A clinical method for mapping and quantifying blood stasis in the left ventricle", J. Biomech. 49 (11) (2016) 2152–2161.

[25] O. Mutlu, H.E. Salman, H. Al-Thani, A. El-Menyar, U.A. Qidwai, H.C. Yalcin, How does hemodynamics affect rupture tissue mechanics in abdominal aortic aneurysm: focus on wall shear stress derived parameters, time-averaged wall shear stress, oscillatory shear index, endothelial cell activation potential, and relative residence time, Comput. Biol. Med. 154 (2023).

[26] A. Qureshi, et al., Modelling virchow's triad to improve stroke risk assessment in atrial fibrillation patients. 2022 Computing in Cardiology (CinC), Tampere, Finland, 2022, pp. 1–4, https://doi.org/10.22489/CinC.2022.378.

[27] A. Qureshi, G.Y.H. Lip, D.A. Nordsletten, S.E. Williams, O. Aslanidi, A. de Vecchi, Imaging and biophysical modelling of thrombogenic mechanisms in atrial fibrillation and stroke, Front Cardiovasc Med 16 (9) (2023) 1074562.

[28] X. Morales, J. Mill, K. Sørensen, C. Acebes, X. Iriart, B. Legghe, H. Cochet, O. De Backer, R. Paulsen, O. Camara, "Deep learning framework for real-time estimation of in-silico thrombotic risk indices in the left atrial appendage", Front. Physiol. 12 (2021).

[29] N. Paliwal, H.C. Park, Y. Mao, S.J. Hong, Y. Lee, D.D. Spragg, H. Calkins, N.A. Trayanova, Slow blood-flow in the left atrial appendage is associated with stroke in atrial fibrillation patients, Heliyon 10 (5) (2024 Feb 28) e26858, https://doi.org/10.1016/j.heliyon.2024.e26858.

[30] A.G. Passerini, D.C. Polacek, C. Shi, N.M. Francesco, E. Manduchi, G.R. Grant, et al., "Coexisting proinflammatory and antioxidative endothelial transcription profiles in a disturbed flow region of the adult porcine aorta", Proc. Natl. Acad. Sci. 101 (2004) 2482–2487.

[31] T. Torisu, K. Torisu, I.H. Lee, J. Liu, D. Malide, C.A. Combs, et al., "Autophagy regulates endothelial cell processing, maturation and secretion of von Willebrand factor", Nat. Med. 19 (2013) 1281–1287.

[32] N. Mackman, "New insights into the mechanisms of venous thrombosis", J. Clin. Invest. 122 (2012) 2331–2336.

[33] E. Melillo, G. Palmiero, A. Ferro, et al., "Diagnosis and management of left atrium appendage thrombosis in atrial fibrillation patients undergoing cardioversion", Medicina (Kaunas) 55 (2019) 511.
[34] S.S. Abdelmoneim, S.T. Mulvagh, "Techniques to improve left atrial appendage imaging", J. Atr. Fibrillation 7 (2014) 1059.
[35] E. Planas, et al., "In-silico analysis of device-related thrombosis for different left atrial appendage occluder settings". Statistical Atlases and Computational Models of the Heart. Multi-Disease, Multi-View, and Multi-Center Right Ventricular Segmentation in Cardiac MRI Challenge. STACOM 2021, in: Lecture Notes in Computer Science, vol. 13131, Springer, Cham, 2022.